Materials Chemistry and Physics 201 (2017) 224–234

Contents lists available at ScienceDirect

Materials Chemistry and Physics

journal homepage: www.elsevier.com/locate/matchemphys

# Piezoelectric sensitivity and hydrostatic response of novel lead-free 2–0–2 composites with two single-crystal components

V. Yu. Topolov [a,*], C.R. Bowen [b], A.A. Panich [c], A.N. Isaeva [a]

[a] Department of Physics, Southern Federal University, 5 Zorge Street, 344090 Rostov-on-Don, Russia
[b] Department of Mechanical Engineering, University of Bath, Bath BA2 7AY, United Kingdom
[c] Institute of High Technologies and Piezotechnics, Southern Federal University, 10 Milchakov Street, 344090 Rostov-on-Don, Russia

## HIGHLIGHTS

- High piezoelectric sensitivity of novel lead-free 2–2-type composites is stated.
- Role of two single-crystal components in forming the high performance is described.
- New aspect-ratio effect is studied to increase hydrostatic parameters of composites.
- Large piezoelectric anisotropy of the 2–2-type composite is first discussed.

## ARTICLE INFO

*Article history:*
Received 30 January 2017
Received in revised form
15 July 2017
Accepted 16 August 2017
Available online 19 August 2017

*Keywords:*
Piezo-active composite
Single crystal
Piezoelectric properties
Hydrostatic parameters
Elastic properties

## ABSTRACT

This paper reports the piezoelectric performance and important related hydrostatic parameters of 2–0–2 composites based on lead-free ferroelectric and piezoelectric single crystals with 4*mm* symmetry. We demonstrate that ferroelectric domain-engineered alkali niobate-tantalate based single crystals provide large values of the piezoelectric coefficients $g_{3j}^*$ and related parameters when used in a 2–0–2 composite system with a relatively wide range of volume fractions of single-crystal components. An 'aspect-ratio effect' as a result of the presence of inclusions of a piezoelectric $Li_2B_4O_7$ single crystal in a polymer medium is studied for the first time for a case where the elastic compliance $s_{12}$ in the single crystal/polymer layer of the composite passes through zero. It is observed that changes in the aspect ratio and volume fraction of the $Li_2B_4O_7$ inclusions influence the hydrostatic piezoelectric coefficient $g_h^*$, squared figure of merit $d_h^* g_h^*$ and electromechanical coupling factor $k_h^*$ of the composite, and large values of $g_h^* \sim 10^2$ mV·m/N, $d_h^* g_h^* \sim (10^{-11}–10^{-10})$ Pa$^{-1}$ and $k_h^* \approx 0.6–0.7$ are achieved. A link between max $k_h^*$ and a change in sgn$s_{12}$ is first described for the 2–2-type composite, and a comparison of the hydrostatic parameters of the novel and related composites is made. The present results show the potential of lead-free 2–0–2 composites that are suitable for piezoelectric sensor, energy-harvesting and hydroacoustic applications.



## 1. Introduction

In the last decades, piezo-active composites based on relaxor-ferroelectric single crystals (SCs), such as $(1-x)Pb(Mg_{1/3}Nb_{2/3})O_3 - xPbTiO_3$ (PMN–*x*PT) and $(1-x)Pb(Zn_{1/3}Nb_{2/3})O_3 - xPbTiO_3$ (PZN–*x*PT) have been developed and studied [1–3] to meet a variety of piezo-technical applications that include sensors, hydrophones, energy-harvesting devices [4,5], etc. The overwhelming majority of SC components that exhibit outstanding electromechanical properties [6,7] are lead-based, and there is concern that these components may pollute the environment because of the toxicity of the chemical element Pb. An important challenge in modern materials science concerned with active dielectrics and their piezo-technical applications is to find an appropriate alternative [8,9] to lead-containing ferroelectric and piezoelectric materials, which are able to replace the well-known PZT-type ceramics [10–12] that are based on the perovskite-type $Pb(Zr, Ti)O_3$ solid solution.

Lead-free ferroelectric solid solutions with the perovskite-type structure are of interest due to their promising piezoelectric

* Corresponding author.
*E-mail address:* vutopolov@sfedu.ru (V.Yu. Topolov).

http://dx.doi.org/10.1016/j.matchemphys.2017.08.041

performance, considerable electromechanical coupling [8–11] and their potential application in a variety of transducer applications [10,13]. For example, ferroelectric ceramics based on alkali niobates [9,10] have become a large group of lead-free materials that are attractive due to their high piezoelectric sensitivity, large piezoelectric anisotropy, figures of merit, and high-power performance [13,14]. Of additional interest are domain-engineered SCs based on alkali niobates-tantalates with optimised electromechanical properties. These SCs are characterised [15–17] by relatively large piezoelectric coefficients $d_{ij}$ and electromechanical coupling factors $k_{ij}$ (ECFs). Examples of the electromechanical properties of the [001]-poled SCs are shown in Table 1. Such SCs can be regarded as an alternative to the widespread conventional lead-containing ferroelectric ceramics, e.g., when absolute values of the piezoelectric coefficients $d_{ij}$ are larger in the lead-free SCs in comparison to the poled polycrystalline lead-based ceramics. Another alternative is concerned with applications where there is a need for high piezoelectric sensitivity and the piezoelectric coefficient $g_{33}$ of the SCs is large in comparison to the moderate values of $g_{33}$ of many poled polycrystalline ceramics. In addition to replacing lead-based bulk materials, new examples of high-performance piezoelectrics can be achieved by using the lead-free SCs as components in modern piezo-active composite configurations [18,19] with 1–3 and 2–2 connectivity patterns.

In recent work [20], a laminar three-component SC/ceramic/polymer composite, which was based on the [001]-poled PMN–0.33PT SC and described by 2–0–2 connectivity in terms of Refs. [4, 21], was found to exhibit a large hydrostatic piezoelectric response. In earlier experimental studies [22], a promising example of a 2–0–2 composite based on a ferroelectric ceramic was demonstrated, and the improved piezoelectric performance of this composite was shown to be a result of an active role of lead-free inclusions present in the polymer layers. However the role of the heterogeneous layer and its active component has yet to be studied in detail. The aim of the present paper is to analyse the piezoelectric performance and hydrostatic parameters of the 2–0–2 composites based on the [001]-poled lead-free SCs and to demonstrate the potential of these novel lead-free composite materials in comparison to the 2–2-type lead-containing composites.

## 2. Model of the 2–0–2 composite, its effective parameters and components

### 2.1. Model of the composite

The 2–0–2 composite consists of a system of parallel-connected layers of two types (*Type I* and *Type II* layers, Fig. 1) with interfaces that are parallel to the ($X_2OX_3$) plane. These layers are regularly arranged along the coordinate $OX_1$ axis. The Type I layer is a ferroelectric domain-engineered SC and is characterised by a spontaneous polarisation $\boldsymbol{P}_s^{(1)}$ and volume fraction $m$. Hereafter we denote this component *SC-1*. Its main crystallographic axes $X$, $Y$ and $Z$ are oriented as follows: $X \parallel [001] \parallel OX_1$, $Y \parallel [010] \parallel OX_2$ and $Z \parallel [001] \parallel OX_3$, where the $[hkl]$ direction is given in the perovskite unit-cell axes. The orientation of the non-180° domains formed in the ferroelectric 3$m$ phase under an electric field $\boldsymbol{E} \parallel OX_3$ is shown in the inset 1 in Fig. 1. At equal volume fractions of these domains, the SC-1 is characterised by 4$mm$ symmetry [6,7,15–17].

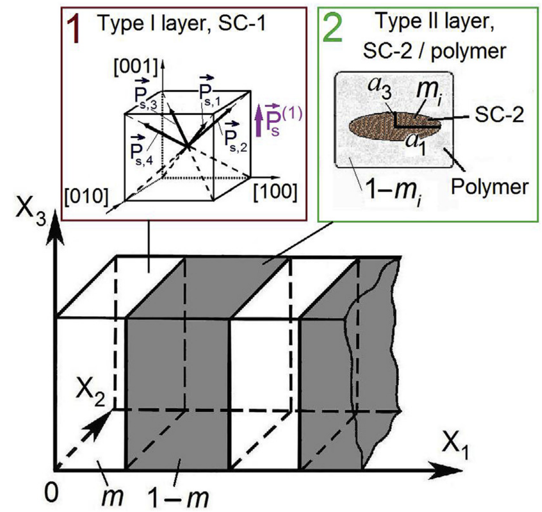


**Fig. 1.** Schematic of the 2–0–2 SC-1/SC-2/polymer composite. ($X_1X_2X_3$) is a rectangular co-ordinate system, $m$ and $1 - m$ are volume fractions of the type I and type II layers, respectively, $\boldsymbol{P}_s^{(1)}$ is the spontaneous polarisation vector of the domain-engineered SC-1 poled along the $OX_3$ axis, $m_i$ is the volume fraction of the SC-2 inclusions in the polymer medium, and $a_1$ and $a_3$ are semi-axes of each inclusion.

The Type II layer is a SC-2/polymer medium with 0–3 connectivity in terms of Ref. [21], and the volume fraction of the Type II layers is $1 - m$ (Fig. 1). The shape of each SC-2 inclusion is shown in the inset 2 in Fig. 1 and obeys the equation $(x_1/a_1)^2 + (x_2/a_1)^2 + (x_3/a_3)^2 = 1$ in the co-ordinate $OX_f$ axes. Hereby $\rho_i = a_1/a_3$ is the aspect ratio of the SC-2 inclusion, and $m_i$ is the volume fraction of the SC-2 in the Type II layer. We assume that the linear sizes of each SC-2 inclusion are much smaller than the thickness of each layer of the composite sample shown in Fig. 1. The SC-2 inclusions occupy sites of a simple tetragonal lattice with unit-cell vectors parallel to the $OX_f$ axes. As with the SC-1, the orientation of the crystallographic axes $X$, $Y$ and $Z$ of each SC-2 inclusion in the Type II layer is given by $X \parallel OX_1$, $Y \parallel OX_2$ and $Z \parallel OX_3$.

### 2.2. Effective properties and hydrostatic parameters of the composite

Effective electromechanical properties of the 2–0–2 composite are evaluated in two stages which will now be described. During the first stage, we calculate the effective electromechanical properties of the Type II layer by regarding it as a 0–3 SC-2/polymer

**Table 1**
Room-temperature elastic compliances $s_{ab}^E$ (in $10^{-12}$ Pa$^{-1}$), piezoelectric coefficients $d_{ij}$ (in pC/N) and dielectric permittivity $\varepsilon_{pp}^\sigma$ of the [001]-poled domain-engineered SC[a] components.

| Components | $s_{11}^E$ | $s_{12}^E$ | $s_{13}^E$ | $s_{33}^E$ | $s_{44}^E$ | $s_{66}^E$ | $d_{31}$ | $d_{33}$ | $d_{15}$ | $\varepsilon_{11}^\sigma/\varepsilon_0$ | $\varepsilon_{33}^\sigma/\varepsilon_0$ |
|---|---|---|---|---|---|---|---|---|---|---|---|
| KNN–T[b] | 11.9 | −4.30 | −5.60 | 15.5 | 12.0 | 10.7 | −77.0 | 162 | 45.0 | 291 | 267 |
| KNN–TL[c] | 17.2 | −5.11 | −10.7 | 27.0 | 15.4 | 13.9 | −163 | 354 | 171 | 1100 | 790 |
| KNNTL:Mn[d] | 33.4 | −7.36 | −25.8 | 57.7 | 12.8 | 13.5 | −260 | 545 | 66 | 400 | 650 |

[a] Data are related to the main crystallographic axes of the SC with macroscopic 4$mm$ symmetry.
[b] $(K_{0.562}Na_{0.438})(Nb_{0.768}Ta_{0.232})O_3$, Ref. [15].
[c] $[Li_x(K_{0.501}Na_{0.499})_{1-x}](Nb_{0.660}Ta_{0.340})O_3$, Ref. [16].
[d] $[Li_x(K_{1-y}Na_y)_{1-x}](Nb_{1-z}Ta_z)O_3$:Mn, where $x = 0.06$, $y = 0.1$–$0.3$, $z = 0.07$–$0.17$, and the level of Mn doping is 0.25 mol. %, Ref. [17].